Articles

Investigation into the Catalytic Role for the Tryptophan Residues within Domain III of *Pseudomonas aeruginosa* Exotoxin A†

Bryan K. Beattie, Gerry A. Prentice, and A. Rod Merrill*

Guelph-Waterloo Centre for Graduate Work in Chemistry, Ontario Department of Chemistry and Biochemistry, University of Guelph, Guelph, Ontario N1G 2W1, Canada

Received August 7, 1996; Revised Manuscript Received September 17, 1996⊗

ABSTRACT: The role of the tryptophan residues in the substrate-binding and catalytic mechanism of an enzymatically active C-terminal fragment of *Pseudomonas aeruginosa* exotoxin A was studied by individually or jointly replacing these residues with phenylalanine. Substitution of W-466 decreased the ADP-ribosyltransferase and NAD^+-glycohydrolase activities by 20- and 3-fold, respectively. In contrast, substitution of W-417 or W-558 with phenylalanine both resulted in a 3-fold decrease in ADP-ribosyltransferase activity with, however, only a decrease by 40% and 70% in NAD^+-glycohydrolase activity, respectively. Simultaneous replacement of W-466 and W-558 resulted in a 200-fold decrease in ADP-ribosyltransferase and an 6-fold decrease in NAD^+-glycohydrolase activities, suggesting that W-466 may play a minor role in the transfer of ADP-ribose to the eEF-2 protein. Chemical modification of the tryptophan residues in the wild-type toxin fragment by *N*-bromosuccinimide revealed the presence of a single residue important for enzymatic activity, W-466, with a minor contribution from W-558. Additionally, tryptophan residues, W-305 and W-417, were refractory to oxidation by *N*-bromosuccinimide, which likely indicated the buried nature of these residues within the protein structure. Titration of the wild-type toxin fragment with NAD^+ resulted in the quenching of the intrinsic tryptophan fluorescence to 58% of the initial value. Titration of the various single and a double tryptophan replacement mutant protein(s) indicated that W-558 and W-466 are responsible for the substrate-induced fluorescence quenching, with the former being responsible for the largest fraction of the observed quenching in the wild-type toxin. Consequently, a molecular mechanism is proposed for the substrate-induced fluorescence quenching of both W-466 and W-558. Furthermore, molecular modeling of the recent crystal structures for both exotoxin A (domain III fragment) and diphtheria toxin, combined with a variety of previous results, has led to the proposal for a catalytic mechanism for the ADP-ribosyltransferase reaction. This mechanism features a S_N1 attack (instead of the previously purported S_N2 mechanism) by the diphthamide residue (nucleophile) of eukaryotic elongation factor 2 on the C-1 of the nicotinamide ribose of NAD^+, which results in an inversion of configuration likely due to steric constraints within the NAD^+−toxin−elongation factor 2 complex.

Pseudomonas aeruginosa is an ubiquitous, Gram-negative bacillus which acts as an opportunistic human pathogen. The premier pathogen of the *Pseudomonas* species, *P. aeruginosa* is a leading cause of infection in burn, cystic fibrosis, postoperative patients and in other various immune-compromised hosts (Vasil *et al*., 1986). *P. aeruginosa* produces a large number of toxic factors that have the potential to contribute to its pathogenicity (Liu *et al*., 1973). The most potent of these virulence factors is the extracellular protein, exotoxin A (ETA).[1]

ETA belongs to a family of toxins related in their mechanisms of action, which include diphtheria toxin (DT), pertussis toxin, cholera toxin, and *Escherichia coli* heat-labile toxin. These toxins exert their effects via ADP-ribosylation of specific target molecules within eukaryotic cells. More specifically, ETA and DT catalyze the transfer of the ADP-ribose moiety of NAD^+ onto elongation factor 2 (eEF-2) (Iglewski *et al*., 1977; Oppenheimer & Bodley, 1981). This covalent transfer inactivates eEF-2, rendering it incapable of polypeptide chain elongation, inhibiting protein synthesis and eventually killing the target cell.

† Supported by the Medical Research Council of Canada (A.R.M.).

* Corresponding author [telephone, (519) 824-4120 ext 3806; fax, (519) 766-1499; E-mail, MERRILL@CHEMBIO.UOGUELPH. CA].

⊗ Abstract published in *Advance ACS Abstracts,* November 15, 1996.

[1] Abbreviations: ADPRT, ADP-ribosyltransferase; CD, circular dichroism; 3-D, three dimensional; DT, diphtheria toxin; DTT, dithiothreitol; eEF-2, eukaryotic elongation factor 2; EDTA, ethylenediaminetetraacetic acid; ETA, *Pseudomonas aeruginosa* exotoxin A; GH, glycohydolase activity; ΔG_s, stabilization free energy of the native folded state; HPLC, high-performance liquid chromatography; IPTG, isopropyl β-D-thiogalactopyranoside; K_s, substrate binding (dissociation) constant; NAD^+, β-nicotinamide adenine dinucleotide (oxidized form); NATA, *N*-acetyltryptophanamide; NBS, *N*-bromosuccinimide; PE40, *P. aeruginosa* exotoxin A 40 kDa C-terminal fragment; PMSF, phenylmethanesulfonyl fluoride; SDS−PAGE, sodium doceyl sulfate−polyacrylamide gel electrophoresis; SpC, specificity constant; TCA, trichloroacetic acid; Tris, tris(hydroxymethyl)aminomethane; Trp_{ox}, number of Trp residues oxidized by NBS treatment; WT, wild type.

S0006-2960(96)01985-X CCC: $12.00

The 3-D crystallographic structure of the 613 kDa amino acid ETA protein has been solved to 3.0 Å resolution (Allured *et al*., 1986). On the basis of the crystal structure of the 66 kDa ETA molecule, along with other physicochemical data, molecular models were proposed that consist of three distinct functional domains. Domain Ia (residues 1−252) is involved in receptor binding, domain Ib (residues 365−404) has no known function, and domain II (residues 253−364) aids in translocation across the endosomal membrane into the host cell cytoplasm after receptor-mediated endocytosis. Domain III (residues 405−613) comprises the catalytic domain which contains an extended cleft postulated to be the active site of the enzyme.

From the resolved 2.3 Å crystal structure of DT (Bennett *et al*., 1994), some active site residues have been located in essentially identical positions within the two toxins. Previously, a model was proposed where NAD^+ fits into the cleft with the adenine ring bound in the hydrophobic pocket defined by the aromatic rings of Tyr 470 (Tyr 54, DT), Tyr 481 (Tyr 65, DT), Trp 466 (Trp 50, DT), Trp 558 (Trp 153, DT), and His 440 (His 21, DT) (Domenighini *et al*., 1991). The model suggests that either the nicotinamide or adenine ring of NAD^+ would stack on the indole ring of Trp 466. Recently, the 2.5 Å crystal structure of domain III of ETA complexed with NAD^+ hydrolysis products (AMP and nicotinamide) has been solved (Li *et al*., 1995), and close inspection of this structure revealed that NAD^+ likely does not directly interact with the Trp 466 side chain (Gerry Prentice, unpublished observation). Furthermore, a 3-D structure of domain III of ETA complexed with a NAD^+ analog has also been determined (Li *et al*., 1996).

Within domain III of ETA are three tryptophans (Trp 417, Trp 466, and Trp 558) which could potentially participate in hydrophobic stacking interactions as previously described. Previous reports indicated that, upon NAD^+ binding to the catalytic domain, the intrinsic protein fluorescence of ETA is quenched by up to 30% (Killeen & Collier, 1992). This effect was attributed to the fluorescence quenching of one or more tryptophans located within domain III. In order to elucidate the roles of these tryptophans in substrate binding and catalysis, we made conservative substitution (phenylalanine for tryptophan) using a site-directed mutagenesis technique. The effects of these mutations were determined by accessibility to *N*-bromosuccinimide (NBS), ADP-ribosyltransferase (ADPRT) activity, NAD^+-glycohydrolase (GH) activity, and NAD^+-binding affinity. The results suggest that Trp 466 plays an indirect role in ADPRT catalysis by maintaining the structural integrity of the active site. Furthermore, both Trp 466 and Trp 588 are responsible for the observed substrate-induced fluorescence quenching effect in the wild-type protein observed upon active site titration with NAD^+. Moreover, molecular modeling studies of the active sites for both ETA and DT were performed on the basis of the new X-ray data available for both structures. The results of these modeling experiments have provided the impetus for a revised catalytic mechanism for the ADPRT reaction catalyzed by ETA.

EXPERIMENTAL PROCEDURES

Chemicals and Enzymes. Restriction endonucleases, T7 DNA polymerase, and T4 DNA ligase were purchased from Pharmacia LKB (Quebec) and New England Biolabs (Mississauga, Ontario). The BL21(λDE3) cells were obtained from Novagen (Madison, WI); isopropyl β-D-thiogalactopyranoside (IPTG) was from Alexis Corp. (San Diego, CA); Q-Sepharose Fast-Flow anion-exchange resin was from Pharmacia-LKB (Quebec); [*adenylate*-^{3}H]NAD^+ was supplied by Dupont, NEN Research Products (Boston, MA); [*adenylate*-^{32}P]NAD^+ and [*nicotinamide*-4-^{3}H]NAD^+ were obtained from Amersham (Oakville, Ontario); and dithiothreitol (DTT) was from Promega Corp. (Madison, WI). The following chemicals were obtained from Sigma Chemical Co. (St. Louis, MO): β-NAD^+, *N*-bromosuccinimide (NBS), Trizma base, bovine serum albumin (BSA), phenylmethanesulfonyl fluoride (PMSF), and wheat germ.

Oligonucleotide-Directed Mutagenesis. Mutagenesis was performed using the Kunkel method as previously described (Steer & Merrill, 1995). Dideoxy sequencing was performed using an ABI Prism Model 377 DNA sequencer using dye termination and cycle sequencing. DNA samples were analyzed in 4.5% acrylamide gels that were 36 cm in length.

Overexpression and Purification of PE40 and Mutants. WT PE40 and mutant proteins were overexpressed in *E. coli* strain BL21(λDE3) cells and purified using a previously described procedure (Beattie & Merrill, 1996). Briefly, 5 μL of plasmid pmS8 (Kondo *et al*., 1988) was transformed into BL21(λDE3) cells, and plated onto four 2 × YT medium plates containing 100 μg/mL ampicillin. Each plate was scraped, and the cells were placed into 50 mL of super L-broth supplemented with 0.04% $MgSO_4$ and 0.5% glucose. The culture was grown at 37 °C to a high cell density (≈1 h), and 10 mL of cell-containing growth medium was transferred to each of four 1 L cultures. These cultures were grown until the cells reached an OD_{650} between 0.5 and 0.7. Subsequently, the cells were induced with IPTG (1 mM) and grown an additional 90 min at 37 °C.

The periplasmic fraction was isolated as previously described (Rasper & Merrill, 1994), and the extract was loaded onto a Q-Sepharose Fast-Flow anion-exchange column, previously equilibrated in 20 mM Tris·HCl, pH 7.6 (buffer A). After the column was washed with approximately 500 mM buffer A, the column was developed with 60 mL of 0.15 M NaCl in buffer A, followed by a second-step gradient consisting of 0.4 M NaCl in buffer A but at pH 7.4. Fractions containing PE40 were pooled, and the effluent was dialyzed overnight in buffer A. The dialyzed sample was concentrated to 5 mL using an Amicon Centriprep concentrator (Amicon Inc., Beverly, MA). This sample was applied to a 1.25 cm diameter × 3.7 cm length HPLC column packed with Q-Sepharose HP (Pharmacia) and eluted with a linear gradient of NaCl (0−500 mM in buffer A; 1 mL/min flow rate) over 120 min. The toxin eluted between 0.20 and 0.25 M NaCl. Fractions containing PE40 were pooled and concentrated to 5 mL using an Amicon Centriprep concentrator, and the HPLC step was repeated at a higher pH (7.8) in buffer A. The final purified protein was concentrated to 2−8 mg/mL, and protein concentration was determined by absorbance using $\epsilon_{M(280)}$ of 4.17×10^4 M^{-1} cm^{-1}, calculated according to the method of Gill and von Hippel (1989). The protein was dispensed into small volume aliquots and frozen at −80 °C. Protein purity was assessed by SDS−PAGE (12.5% gels stained with Coomassie Brilliant Blue; Laemmli, 1970). Furthermore, PE40 was identified by Western blot analysis using a polyclonal

antibody to whole toxin (ETA) as previously described (Rasper & Merrill, 1994).

Purification of eEF-2. Wheat germ was used as the source of eEF-2 protein, and the procedure was a modification of previous procedures (Nilsson & Nygaard, 1984; Carroll & Collier, 1988). One hundred grams of wheat germ (untreated) was suspended in 50 mM Tris·HCl buffer, pH 8.0, containing 5 mM magnesium acetate, 5 mM β-mercaptoethanol, 4 mM $CaCl_2$, 100 mM KCl, and 1 μg/mL PMSF and was then homogenized in a Waring blender (4 × 15 s). The homogenate was centrifuged for 15 min at 21000*g*, the supernatant removed, the pH adjusted to 7.6 with 0.1 M Trizma base, and the solution was centrifuged as before. The supernatant was then subjected to ultracentrifugation at 250000*g* for 60 min. The eEF-2 protein was precipitated from the 30−50% $(NH_4)_2SO_4$ fraction, and the pellets (containing eEF-2) were recovered by centrifugation for 15 min at 21000*g*. The pellets were resuspended in 20 mM Tris·HCl (pH 7.6) containing 1 mM EDTA, 1 mM DTT, 5% glycerol, 1 μg/mL PMSF (buffer B) and 100 mM KCl. The solution was then dialyzed against two changes of buffer B. Precipitated protein was removed by low-speed centrifugation as before. The supernatant was applied to a DEAE-Sephacel column (2.5 diameter × 14 cm length) equilibrated with 20 mM Tris·HCl buffer (pH 7.6) containing 0.1 mM EDTA, 1 mM DTT, 5% glycerol, 1 μg/mL PMSF (buffer C), and 100 mM KCl. The eEF-2 protein was eluted with a single step gradient of buffer C containing 150 mM KCl. The eluted protein fractions were pooled and dialyzed against buffer C and 50 mM KCl, followed by loading to a precycled and equilibrated phosphocellulose column (2.5 cm diameter × 15 cm length). The eEF-2 fraction was eluted with a step gradient of buffer C containing 200 mM KCl. It was determined by SDS−PAGE analysis that the eEF-2 was greater than 90% pure. The eEF-2 protein fraction was concentrated to 10−20 mg/mL and filtered through a 0.2 μm Acrodisc membrane filter (13 mm diameter, Gelman Scientific, Rexdale, Ontario), and it was dispensed into small aliquots and then frozen at −80 °C.

Oxidation of Tryptophans in PE40 with NBS. The modification of PE40 with NBS was accomplished in 50 mM sodium acetate, pH 6.0, at 25 °C in a total volume of 600 μL with an initial A_{280} for various proteins between 0.4 and 0.7. The degree of oxidation of the tryptophans was calculated from the expression (Spande & Witkop, 1967):

$$\mathrm{Trp_{ox}} = \frac{(\Delta \mathrm{Abs_{280nm}})(1.31)}{[\mathrm{protein}](2779.5)}$$

where 1.31 corrects for the absorption change at 280 nm of the oxidation product of tryptophan, oxindole (Spande & Witkop, 1967), and 2779.5 is the molar extinction coefficient at 280 nm for tryptophan using a 0.5 cm path-length cuvette. For analysis of the ADPRT activity at various values of Trp_{ox}, 5.0 μL aliquots were removed and assayed as described later. Trp_{ox} values were corrected for volume changes after aliquot removal and represent the mean of three to four separate experiments.

ADP-ribosyltransferase Assay. Samples were assayed for ADP-ribosylating activity essentially as described by Wilson *et al*. (1994). [*adenosine*-^{32}P]NAD^+ (1000 Ci/mmol, Amersham) was diluted to a final specific activity of 1 Ci/mmol with unlabeled NAD^+ to give a final concentration of 2 mM. The final concentrations of toxin used in the reactions were 21, 64, 819, and 78 pM for wild-type, W417F, W466F, and W558F proteins, respectively, and 5.8 nM for the W466F/W558F protein. Duplicate reactions in a final volume of 26.5 μL consisting of 20 mM Tris·HCl, pH 8.2, containing 1 mM EDTA, 20 mM DTT, 50 μg/mL BSA, NAD^+ (25−500 μM), and 2.5 μM eEF-2 were incubated with the toxin at 25 °C for up to 4 min. Aliquots (6.0 μL) were removed at 1 min intervals and applied to Whatman 3MM paper (1-in. squares) saturated in 10% trichloroacetic acid (TCA) (in ether), then washed four times for 15 min each with 5% TCA (in doubly distilled H_2O) and twice with methanol for 5 min each, air-dried, and counted with 10 mL of ICN CytoScint in a Beckman LS 6000SE scintillation counter. The kinetic parameters were obtained by analysis of Eadie−Hofstee and Hanes−Woolf plots of initial rates for ADP-ribosylation under conditions where eEF-2 was not concentration limited.

NAD^+-glycohydrolase Assay. Samples were assayed for GH activity essentially as described by Wilson *et al*. (1994). [*nicotinamide*-4-^{3}H]NAD^+ (1.2 Ci/mmol, Amersham) was diluted to a final specific activity of 50 Ci/mol with unlabeled NAD^+ to give a final concentration of 1 mM. To determine the specific activities, the reactions were repeated for four different concentrations of each protein, with final concentrations of toxin used in the reactions being 0.6, 0.8, 1.0, and 1.2 μM for wild type and W417F; 1.6, 2.2, 2.8, and 3.4 μM for W466F; 1.2, 1.6, 2.0, and 2.4 μM for W558F; and 4.0, 5.4, 6.8, and 8.2 μM for W466F/W558F. Duplicate reactions were performed at 100 μM NAD^+ in the presence of toxin at 25 °C for up to 4 h, in a final volume of 200 μL of 50 mM Tris·HCl, pH 8.2, containing 10 mM DTT, 1 mM EDTA, and 50 μg/mL BSA. Aliquots (45 μL) were removed at 1 h intervals followed by transfer to 10 μL of 1 M boric acid, pH 8.0, and extraction with 200 μL of water-saturated ethyl acetate. Aliquots (160 μL) of the organic phase were removed and counted with 3 mL of ICN CytoScin in an Beckman LS 6000SE scintillation counter. Furthermore, the data were corrected for nonenzymatic hydrolysis of NAD^+. Specific activities for NAD^+-glycohydrolysis were determined from the reaction rates obtained as a function of enzyme concentration and were V_{max} values (data not shown).

Quenching of Intrinsic Protein Fluorescence. The NAD^+-dependent quenching of intrinsic protein fluorescence was monitored as a function of the concentration of NAD^+. Duplicate reactions were performed over a concentration range of 0−750 μM NAD^+ in the presence of toxin at 25 °C in an initial volume of 750 μL of 50 mM Tris·HCl, pH 8.2. Samples were excited at 295 nm (4-nm band-pass), and the fluorescence intensity was measured over the range of 305−400 nm (4-nm band-pass) in a computer-controlled PTI Alphascan-2 spectrofluorometer (Photon Technology Inc., South Brunswick, NJ). The final concentrations of toxin used in the experiments were 0.8 μM wild type; 1.0 μM W417F, W466F, and W558F; and 1.33 μM W466F/W558F. The fluorescence intensity of *N*-acetyltryptophanamide (NATA) as a function of NAD^+ concentration was used to correct for the absorptive screening by NAD^+ at the excitation wavelength. The differences in binding energies for NAD^+ in the binary toxin−NAD^+ complex were determined from the dissociation constants (K_s) obtained from fluorescence quenching measurements according to the equation $\Delta G_s = RT \ln K_s$.

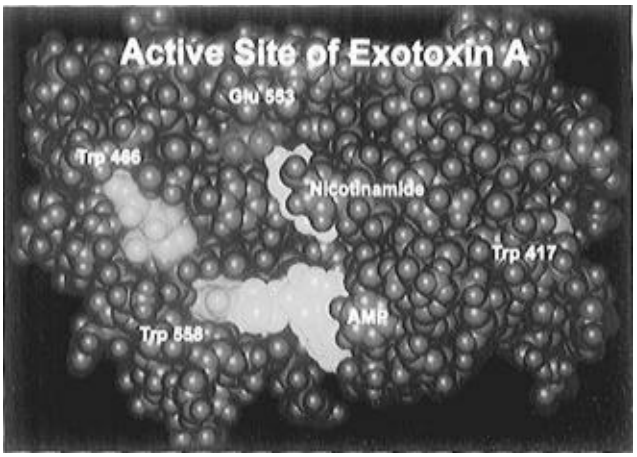

FIGURE 1: Space-filling model for domain III of ETA. The three tryptophans in domain III are indicated in green. The catalytically important glutamic acid residue is shown in red. The results of NAD^+ hydrolysis, nicotinamide and AMP, are colored in yellow. The space-filling diagram was generated using Biosym Insight II from the 2.5 Å refined X-ray structure (Li *et al*., 1995).

Molecular Modeling Experiments. Molecular modeling experiments on the domain III fragment of ETA (Li *et al*., 1995) and DT (Bell & Eisenberg, 1996) X-ray structures were performed on an IBM RISC System 6000 computer workstation using the Biosym Insight II software package. The crystal structure for ETA domain III consists of a dimer with structure **A** complexed with the nicotinamide fragment of NAD^+ and structure **B** with both AMP and the nicotinamide fragment. Some regions resolved within one monomerwere unresolved in the other and *vice versa*; all shared atoms were superimposed to give overlapping structures. The catalytic domain of DT was excised from the coordinate file supplied by Dr. David Eisenberg, and the resulting file consisted of this domain complexed with intact NAD^+. Initially, all resolved protein atoms for DT were superimposed onto those of structure **B** of ETA domain III. From this alignment, the segments of backbone shared between the toxins were determined and used to realign the catalytic site structures by superimposing the following: the common backbone segments, residues W-466 (W-50, DT), W-558 (W-153, DT), Y-470 (Y-54, DT), Y-481 (Y-65, DT), E-553 (E-158, DT), and H-440 (H-21, DT), and the shared ring and sugar fragments of AMP, nicotinamide, and NAD^+. The spatial arrangement of all three structures provided for the identification of patterns for conformational changes introduced by substrate binding, for comparison of structural features between similar regions, and for determination of potential toxin−substrate interactions in ETA on the possible interactions observed in DT.

RESULTS

Space-Filling Model of the Active Site. Figure 1 shows the active site of ETA as viewed from the mouth of the cleft and is based on the X-ray structure of Li *et al.* (1995). The Trp residues are shown in green and the catalytically important residue, Glu 553, is shown in red. The hydrolysis products of the enzyme's nucleotide substrate, NAD^+, are shown in yellow and include AMP and nicotinamide. One of the ribose phosphate moieties (nicotinamide side) of NAD^+ is absent and likely diffused from the active site domain upon hydrolysis of both the glycosidic and phosphoanhydride bonds of NAD^+ during the crystallization process. Neither Trp 417 nor Trp 466 are sufficiently close to the substrate hydrolysis products to warrant a consideration of direct noncovalent interactions with substrate during catalysis. However, Trp 558 appears to be juxtaposed with the adenine ring of the substrate in which the C-5 and C-6 of its indole ring face the C-2 and N-3 of the purine ring (ca. 3.7 Å apart). Trp 558 is positioned even closer (2−3 Å) to the nicotinamide phosphate (although absent in the X-ray complex, a comparison with the recently solved DT−NAD^+ complex confirmed this observation; Bell & Eisenberg, 1996).

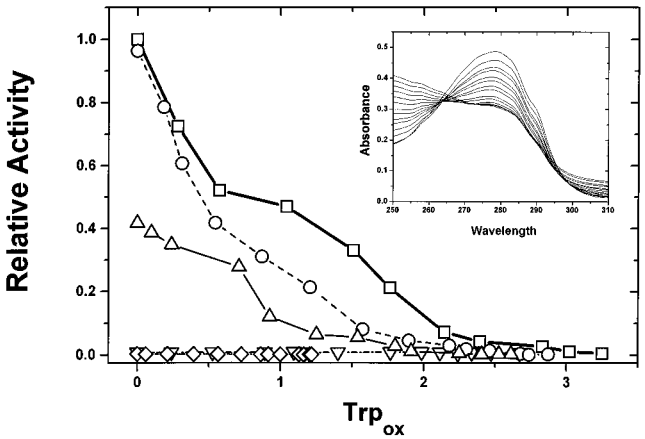

FIGURE 2: Effect of *N*-bromosuccinimide on tryptophans in domain III of PE40. Wild-type and mutant proteins were titrated with NBS, and the number of tryptophans oxidized (Trp_{ox}) was calculated as shown in Table 1. Aliquots were taken at various Trp_{ox} values and assayed for ADPRT activity as described in Experimental Procedures. The samples included WT (□), W417F (○), W466F (▽), W558F (△), and W466F/W558F (◇). To ascertain enzymatic activity, at various stages in the NBS titration, samples were incubated for 2 min at 25 °C with 7.7 μCi of [*adenylate*-^{32}P]NAD^+ (1000 Ci/mmol, 400 μM NAD^+) and wheat germ eEF-2, prepared as described by Carroll and Collier (1987), in 50 mM Tris·HCl, pH 8.2, 1 mM EDTA, and 1 mM DTT (26.5 μL, final volume). Specific activity for wild-type PE40 was 372 mol of NAD^+ min^{-1} (mol of enzyme)$^{-1}$. Inset: Plot of absorbance versus wavelength for the titration of WT PE40 protein with the addition of 0, 20, 35, 45, 55, 65, 75, 85, 100, 115, 130, 145, 160, and 180 nmol of NBS (600 μL, total volume). Measurements were completed on samples from three independent experiments.

Oxidation of Tryptophan with N-Bromosuccinimide (NBS). NBS has proved to be a useful reagent for the determination of the number of Trp residues in proteins (Spande & Witkop, 1967; Clarke, 1987). Figure 2 shows the effect of NBS-induced oxidation of Trp residues on the relative catalytic activity of WT and mutant PE40 proteins (the absorption spectra for a typical NBS titration of WT PE40 is shown in the inset). Titration of the WT PE40 protein with NBS indicated that the oxidation of the equivalent of 2 mol of Trp/mol of enzyme resulted in a catalytically inactive protein. Upon titration with NBS, W417F was the most similar of the mutant proteins to the WT protein. In contrast, the W558F peptide exhibited a titration profile in which its overall activity was reduced compared with the WT and that extrapolated to a single oxidized Trp residue per enzyme molecule. Both W466F and the double mutant, W466F/W558F, showed very low catalytic activities, and their enzymic activities were insensitive to NBS oxidation. Table 1 lists the results from the NBS titration experiment for the WT, four single-substitution PE40 mutant proteins, and one double-replacement mutant (there are two Trp residues at positions 281 and 305 within domain II). The number of

Table 1: Oxidation of Tryptophan in PE40 by *N*-Bromosuccinimide

protein	Trp_{ox}[a]	no. of Trp protected by structure[b]	no. of Trp oxidized[c]
wild type (N)[d]	3.29 ± 0.23	2	3
wild type (D)[d]	4.60 ± 0.12	0	5
W281F	2.30 ± 0.11	2	2
W305F[e]	ND[f]	ND	ND
W417F	2.84 ± 0.18	1	3
W466F	2.49 ± 0.26	2	2
W558F	2.55 ± 0.16	2	2
W466F/W558F	1.34 ± 0.12	2	1

[a] Determined from the decrease in Abs_{280nm} upon formation of the oxidation product of tryptophan as described in Experimental Procedures. Assays were performed as described by Spande and Witkop (1967). The data were collected from three independent experiments for each protein. [b] Approximate determination of the number of tryptophans protected by the structure of the protein determined from the difference between the number of tryptophans oxidized in the denatured wild-type protein and the number of tryptophans oxidized as described in footnote *c*. [c] Approximate number of tryptophans oxidized by NBS as described in footnote *a*. [d] Wild-type PE40 contains five tryptophans. Native (N) and denatured (D) (in 6 M urea) wild-type PE40 were assayed for comparison. [e] W305F could not be purified in sufficient quantities for NBS titration. [f] ND (not determined).

Table 2: Kinetics of ADP-ribosyltransferase Activity for Wild-Type and Mutant PE40 Enzymes[a]

protein	k_{cat} (min^{-1})	rel k_{cat}	K_M (μM) (NAD^+)	k_{cat}/K_M (10^7 M^{-1} min^{-1})	rel k_{cat}/K_M
wild type	1678 ± 385	1	90 ± 32	1.86 ± 0.24	1.0
W417F	639 ± 147	0.38	65 ± 17	1.08 ± 0.44	0.58
W466F	90 ± 51	0.05	159 ± 134	0.07 ± 0.004	0.04
W558F	503 ± 95	0.30	162 ± 64	0.39 ± 0.024	0.21
W466F/ W558F	8 ± 2	0.005	249 ± 100	0.004 ± 0.001	0.002

[a] Assays were performed as described by Wilson *et al*. (1994). The kinetic parameters were determined as described in Experimental Procedures. Kinetic parameters represent the mean ± SD from three to four independent experiments each performed in duplicate.

Trp residues in each protein that was susceptible to NBS oxidation was calculated as described in the Table 1 legend. There were three NBS-sensitive residues for the WT and W417F proteins and two such residues for W281F, W466F, and W558F proteins. A single Trp residue or the equivalent was sensitive to NBS oxidation in the W466F/W558F mutant protein. This implies that two Trp residues are refractory to NBS oxidation in the WT protein. Two Trp residues were also refractory to NBS oxidation in the W281F, W466F, W558F, and W466F/W558F mutant proteins. A single Trp residue was insensitive to NBS oxidation in the W417F protein. As a control to evaluate the usefulness of the NBS titration method, native WT PE40 (five Trp residues) yielded three oxidizable Trp residues (Table 1). Furthermore, in the presence of 4 M urea, this value increased to five oxidizable Trp residues for the denatured protein.

Enzyme Activity of Trp Mutants. The kinetic parameters for the WT and the Trp mutants of PE40 are shown in Table 2. The WT protein showed a turnover number (k_{cat}) of nearly 1700 min^{-1} with a K_M value of almost 100 μM and a specificity constant (k_{cat}/K_M) close to 2×10^7 M^{-1} min^{-1}. Individual substitution of each of the three Trp residues located within the active site of PE40 resulted in a reduction in the k_{cat} values. Replacement of Trp residues, 417 or 558, produced enzymes that possessed approximately one-third of the WT turnover number. However, substitution of Trp 466 with Phe resulted in an enzyme with only 6% the catalytic power of the WT protein. Simultaneous replacement of both Trp residues, 466 and 558, yielded a double mutant protein that possessed less than 1% of the catalytic ability of the WT protein. Interestingly, the K_M values were affected to a lesser extent by Trp → Phe replacement. The only mutation that yielded a mutant enzyme with a significantly altered K_M was the W466F/W558F double mutant; its K_M value was increased 2.5-fold. Nonetheless, the specificity constants (k_{cat}/K_M, SpC), which indicate the ability of the enzyme to work at low substrate concentration, were largely affected by Phe substitution of the Trp residues within the enzyme's catalytic domain due mostly to the altered k_{cat} values. As aforementioned, the WT SpC was 1.86×10^7 M^{-1} min^{-1}, and upon Trp substitution the mutant enzyme, W417F, decreased to 58% of the WT value. Individual substitution of Trp 558 and Trp 466 with Phe resulted in proteins with 21% and 4% of the WT SpC value, respectively. Furthermore, simultaneous replacement of both Trp 466 and Trp 558 resulted in a protein that possessed only 0.2% of the WT SpC value.

Structural Integrity of Trp → Phe Mutants. The structural integrity of the Trp → Phe replacement mutant proteins was tested by CD spectroscopic analysis and by limited proteolytic digestion with trypsin (data not shown). There were negligible changes in the secondary structure for any of these mutant proteins that could be detected by altered secondary structure from CD analysis. It is noteworthy that the variation of ellipticity values for the different proteins was within the error for the determination of the protein concentration by absorption measurements. Furthermore, limited proteolysis of the purified mutant proteins with trypsin revealed no significant alteration in these proteins' sensitivity to proteolysis (data not shown). Also, production of each mutant, including the double Trp → Phe mutant protein, resulted in proteins that expressed and purified similarly to the WT protein (data not shown), which adds further evidence as to the nonperturbing nature of these Trp → Phe substitutions.

Fluorescence Quenching of Trp Fluorescence and NAD^+ Substrate Binding. The titration of WT and mutant PE40 proteins with NAD^+ substrate is shown in Figure 3. Titration of WT PE40 resulted in a 42% reduction of the initial Trp fluorescence (Table 3, Figure 3). Replacement of each of the three Trp residues within the catalytic domain followed by titration with NAD^+ revealed that substitution of both Trp 466 and Trp558 residues alleviated the substrate-induced fluorescence quenching (Figure 3). However, neither the specific nature of the substrate-induced fluorescence quenching mechanism nor the Trp residue(s) within ETA responsible for this phenomenon have been previously identified (Wilson & Collier, 1992). In order to further investigate this quenching mechanism, titration of a number of Trp-replacement mutant proteins with NAD^+ was conducted. When Trp 558 was replaced with Phe in the PE40 protein's active site, the alleviation of the observed quenching upon NAD^+ binding was the largest among the proteins tested. The largest effect was observed upon substitution of Trp 558 (a change from 42% to 25% quenching). The relief in the fluorescence quenching was smaller but significant for the W466F mutant (42% to 36% quenching), whereas there was little or no effect on substrate-induced fluorescence quench-

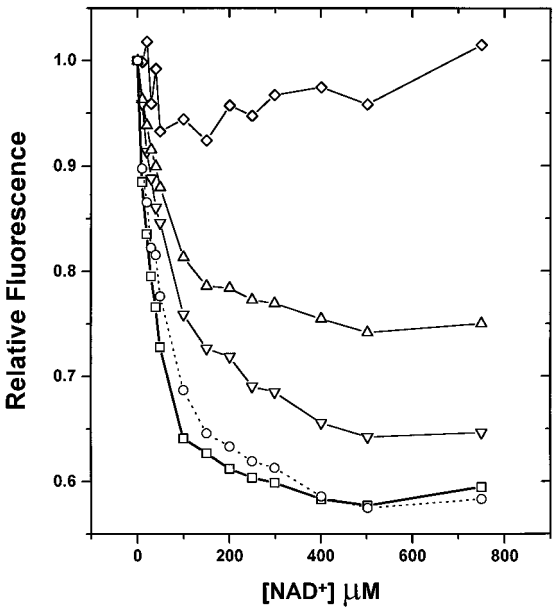

FIGURE 3: Quenching of intrinsic protein fluorescence by NAD^+. Assays were performed as described by Wilson *et al.* (1994). Samples included WT (□), W417F (○), W466F (▽), W558F (△), and W466F/W558F (◇). The fluorescence intensity was corrected for absorptive screening by NAD^+, and the conditions for the fluorescence titration experiment are described in Experimental Procedures. The percent quenching at each NAD^+ concentration was calculated from the data and analyzed by Scatchard plots to determine the dissociation constants, and the K_s values obtained are summarized in Table 4. Results shown are the mean of three independent experiments.

Table 3: Comparison of Dissociation Constants and Interaction Energies for NAD^+ Binding to Wild-Type and Mutant PE40 Proteins

	λ_{max}[a] (nm)	K_s (μM) (NAD^+)[b]	difference in binding energies[c] [$\Delta\Delta G_s$, (kJ/mol)]	% Trp fluorescence quenching at 500 μM[d]
wild type[e]	328	32 ± 2		42
W281F	326	77 ± 5	2.2	40
W305F	330	81 ± 6	2.3	38
W417F	330	41 ± 4	0.6	43
W466F	328	75 ± 3	2.1	36
W558F	332	64 ± 6	1.7	25
W466F/W558F	332	ND[f]	ND	4

[a] Fluorescence emission maxima upon 295 nm excitation. [b] Determined from Scatchard analysis of the percent fluorescence quenching as a function of NAD^+ concentration from footnote *a*; values represent the mean ± SD from three independent experiments. [c] Determined from the difference in the Gibbs free energy, $\Delta G_s = RT \ln K_s$, obtained for NAD^+ binding to the wild-type and mutant proteins. [d] Estimated from the maximum level of fluorescence quenching that occurred as described in footnotes *a* and *b*. [e] The binding energy for the dissociation of the WT protein−NAD^+ complex was 25.6 kJ/mol. [f] Not determined; an estimate from fluorescence quenching measurements was not possible since both reporter groups, Trp 466 and Trp 558, had been replaced with Phe residues.

ing upon replacement of Trp 417 with Phe (W281F was also identical to the WT protein, data not shown; Figure 3). These results were verified by NAD^+ titration of the double mutant protein where both Trp residues, 466 and 558, were replaced with Phe. This mutant protein exhibited little or no significant Trp quenching (ca. 4%) upon titration with as much as 750 μM NAD^+. Notably, a control was used in order to correct for any absorptive screening at the excitation wavelength (295 nm) caused by NAD^+ upon titrating a solution of NATA (at the same concentration as the Trp in the various proteins) with nucleotide substrate. These data were used to provide correction factors at the higher nucleotide concentrations (data not shown), and the data shown in Figure 3 are corrected for this effect. Moreover, it is also important to note that these quenching effects do not take into account the quantum yield of the individual Trp residues, which are not known, but only reveal the relative quenching within each protein.

Table 4: Comparison of Specific Activities for NAD^+-glycohydrolase by Wild-Type and Mutant PE40 Enzymes[a]

protein	k_{cat} ($min^{-1} \times 10^{-2}$)	relative specific activity
wild type	3.07 ± 0.72	1.0
W417F	1.92 ± 0.13	0.62
W466F	0.98 ± 0.11	0.32
W558F	1.03 ± 0.07	0.34
W466F/W558F	0.50 ± 0.17	0.16

[a] Determined from the rates of reaction for NAD^+-glycohydrolysis at 25 °C and pH 8.1 in the presence of 100 μM NAD^+. Assays were performed as decribed by Wilson *et al.* (1994). Values represent the mean ± SD for two independent experiments from duplicate samples.

Substrate Binding Constants and Energies. Titration of the various mutant proteins with NAD^+ allowed for the calculation of the binding constants and energetics of association of the enzyme and its nucleotide substrate (Table 3). The dissociation constant (K_s) for the WT was 32 ± 2 μM, which corresponds to a dissociation energy of 25.0 kJ/mol. The strength of the association of enzyme with substrate modestly decreased (dissociation constant increased) when Trp residues were replaced with Phe in PE40 ($\Delta\Delta G_s$ values ranged from 0.6 to 2.3 kJ/mol). Moreover, when both Trp residues 466 and 558 were substituted with Phe, it was not possible to determine the binding constant by the fluorescence titration method (Table 3, Figure 3). However, GH activities provided an indirect measure of the enzyme−substrate association for the double-mutant (Table 4).

NAD^+-glycohydrolase Activities. The ability of WT and the Trp mutant proteins to hydrolyze NAD^+ in the absence of eEF-2 was measured, and the results are shown in Table 4. This approach is useful in order to give a measure of the structural integrity of the NAD^+-binding pocket. It also serves as an indirect measure of the affinity of the WT and various mutant proteins for the NAD^+ substrate. The WT PE40 exhibited a GH catalytic activity (k_{cat}) of 3.07×10^{-2} min^{-1}, which compares favorably with the GH k_{cat} value for DT (5.6×10^{-3} min^{-1}; Wilson *et al.*, 1994). W417F showed a slightly decreased intrinsic ability to hydrolyze substrate whereas both W466F and W558F showed an even more reduced GH activity than the WT protein (ca. one-third the WT activity). However, the double mutant possessed the poorest GH specific activity (16% of WT activity) but, nonetheless, was still capable of significant GH activity.

DISCUSSION

Careful inspection of the ETA C-domain−AMP/nicotinamide (C-domain-A/N) complex (Li *et al.*, 1995) indicates that the adenine ring of NAD^+ binds in a hydrophobic pocket, and within this nonpolar shell, Trp 558 interacts with the adenine moiety. This interaction was recently described (for

Trp 153) in the DT−NAD^+ complex of Bell and Eisenberg (1996). It is noteworthy that there is a common core fold of approximately 100 residues that contains the NAD^+ binding site that exists for ETA, DT, pertussis toxin, and *E. coli* heat-labile enterotoxin. Interestingly, this NAD^+ binding pocket is seen in ETA (Li *et al*., 1995), and DT (Bell & Eisenberg, 1996) represents a new structural motif for binding this nucleotide cofactor that is unique among this family of toxins and is unlike the Rossmann fold that is characteristic of the dehydrogenases. Importantly, this common fold region for ETA and DT is structurally indistinguishable (Bell & Eisenberg, 1996). In contrast with Trp 558, neither Trp 417 nor Trp 466 is positioned sufficiently close to the NAD^+ substrate to consider a direct interaction. This is clearly observed in both the C-domain−A/N complex and in the DT−NAD^+ complex. Upon NAD^+ binding to both ETA and DT, the intrinsic fluorescence is strongly quenched (Kandel *et al*., 1974; Chung & Collier, 1977; Wilson *et al*., 1990, 1994), but the origin and hence the mechanism of this substrate-induced deactivation of Trp fluorescence are unknown. However, the data shown in Figure 3 clearly indicate that the fluorescence of both Trp 466 and Trp 558 is quenched upon NAD^+ binding, with the latter accounting for the greater part of the quenching process. It is well-known that indole forms ground state complexes with nucleic acid bases (Creed, 1984), and such an indole−adenine complex could explain, at least in part, the observed fluorescence quenching of Trp 558 upon NAD^+ binding.

In contrast, substrate-induced fluorescence quenching of Trp 466 must be accounted for on the basis of an active site side chain quenching mechanism that is triggered by a protein structural change. Upon substrate binding, a significant change in active site structure is seen predominantly in a large loop region, residues 39−46 in DT (Bell & Eisenberg, 1996) and residues 456−470 in ETA (Gerry Prentice, unpublished observation). Located within this loop in the ETA structure are two Asp residues, D-461 and D-463. This loop region is disordered in the substrate-free enzyme (Allured *et al*., 1986) but is visible in both the C-domain−A/N and the DT−NAD^+ complexes. Modeling studies in our laboratory place the carboxyl groups of these two Asp residues within 6−7 Å from the pyrrole ring (N-1) of Trp 466 and upon substrate binding could act through an electron transfer mechanism to deactivate this indole's fluorescence (Creed, 1984). Alternatively, an electrostatic interaction between the ionized carboxyl groups (in the pH range from 7 to 8) of Asp 461 and Asp 463 could lead to the observed fluorescence deactivation of Trp 466. Furthermore, there are also three Arg residues within this loop (Arg 456, Arg 458, and Arg 467), and the guanidino side chain of Arg is known to be an efficient quencher of indole fluorescence but through a largely unknown mechanism (Permyakov, 1993).

The results obtained from the NBS oxidation of the Trp residues in WT PE40 and the various Trp mutants (Figure 2, Table 1) indicate that there are two Trp residues that are refractory to chemically induced oxidation in the WT protein. Considering the various combinations possible and by inference, these two residues are Trp 417 and Trp 305. Molecular modeling studies of the C-domain−A/N complex revealed that Trp 417 is largely buried within the structure in a nonpolar pocket and Trp 305 is also in a largely nonpolar region sandwiched between helices within domain II of ETA (observed in the 2.7 Å partially refined structure; Gerry Prentice, unpublished observation). This observation is supported by the red shift in the fluorescence emission spectra for these proteins upon replacement of the corresponding Trp residues with Phe (Table 3). Furthermore, titration of the various proteins with NBS indicated that two Trp residues, W-466 and W-558, contribute to the catalytic activity of the WT enzyme. This is based on the result shown in Figure 2 that, after NBS titration of the equivalent of 2 mol of Trp residues/mol of protein, both the WT and W417F proteins possessed only residual activity whereas the W558F protein was catalytically inactive after titration of 1 mol of Trp/mol of enzyme. However, initially W466F exhibited very low catalytic activity, indicating that the W466 contributes to a larger extent toward the ADPRT activity of the enzyme. Notably, W466F did show some catalytic sensitivity to NBS oxidation but on a much more reduced scale (Figure 2). Not surprisingly, the double mutant protein was catalytically inactive and enzymatically unresponsive to NBS oxidation.

The K_M parameters for Trp replacement mutants were largely unaltered when compared to the WT enzyme (Table 2). Interestingly, the values obtained for WT ETA (Table 2) compared favorably with previous results reported for DT (1400 min^{-1}, 11.5 μM, and 1.2×10^8 M^{-1} min^{-1} for k_{cat}, K_M, and SpC, respectively; Wilson *et al*., 1994). Notably, a significant effect on the catalytic rate of the enzyme upon Trp replacement was seen for W466F (20-fold decrease) with only marginal effects observed for W417F and W558F. However, the effect was cumulative for the double mutant, W466F/W558F, where the catalytic rate decreased by 200-fold. These changes were largely reflected in the SpC values seen for these mutations. These data indicate that W-466 is the most important catalytic Trp residue with W-417 and W-558 playing a much more minor role. One might speculate that a double mutant, W417F/W466F, would also be catalytically defective, although this mutation was not prepared for this study. Thus, Trp 466 likely plays an indirect role in the catalytic mechanism of the enzyme possibly in maintaining the active site integrity. However, the W → F substitution of 466 resulted in a greater effect on the ADPRT reaction than on the GH activity, suggesting that Trp 466 may play a minor role in the transfer of ADP-ribose to eEF-2 or in helping to effectively dock the translation factor protein on the surface of the ETA−NAD^+ complex. Bell and Eisenberg (1996) suggested that Trp 50 in DT (Trp 466 in ETA) plays only an indirect role in NAD^+ binding, likely acting as an anchor that stabilizes the loop containing Tyr 54 (Tyr 470 in ETA) which packs against the pyridine ring of NAD^+.

The WT enzyme possessed the highest affinity for the NAD^+ substrate whereas all of the Trp replacement mutants exhibited higher K_s values. However, the effect of the replacement of a single Trp on K_s was not dramatic. The determination of the K_s value for the double mutant, W466F/W558F, by fluorescence titration was not possible since the reporter groups (Trp 466 and Trp 558) were absent in this mutant protein. However, the GH activities indicate that productive binding in the double mutant was only moderately affected since this protein possessed 16% of the WT GH activity (Table 4). Furthermore, the K_M value for the double mutant was only slightly higher than for the WT enzyme (Table 2, 90 ± 32 μM; cf. 249 ± 100 μM), adding further

credence to the concept that simultaneous replacement of both Trp 466 and Trp 558 does not substantially alter the ability of the enzyme to interact with its nucleotide substrate. However, the effect of simultaneous Trp replacement was much more attenuated on the catalytic activity where the residual activity was only 0.5% of the WT value (Table 2), suggesting the requirement for precise positioning of NAD^+ in the enzyme's binding pocket for productive and efficient nucleophilic attack by the eEF-2 diphthamide moiety.

Michel and Dirkx (1977) examined the catalytic role of the Trp residues, Trp 50 and Trp 153, in DT fragment A through chemical modification by 2-hydroxy-5-nitrobenzyl bromide. These investigators reported that Trp 153 was critical for ADPRT activity and concluded that this residue was concerned with binding eEF-2 or with the catalytic mechanism. Unfortunately, these researchers were unable to combine the powerful insightful approach of site-directed mutagenesis to complement their chemical modification study as reported in the present study.

Wilson *et al.* (1994) mutated the two active site Trp residues of DT, Trp 50 and Trp 153. These residues in DT correspond to Trp 466 andTrp 558 in ETA, respectively. In their study, Wilson and colleagues replaced each of the Trp residues individually or jointly with phenylalanine or alanine and evaluated these effects on the ADPRT, GH, and substrate binding levels. Replacement of Trp 50 with Ala substantially decreased both ADPRT and GH activities of DT. However, replacement of Trp 153 with Ala resulted in less dramatic effects on these activities. Replacement of either Trp with Phe had only a marginal effect on ADPRT and GH activities, but simultaneous aromatic residue substitution at both Trp sites caused a substantial decrease in the k_{cat} and consequently SpC values. It was concluded that Trp 50 is a major determinant of NAD^+ affinity. Notably, none of the mutations caused any gross structural changes in the mutant proteins as probed by protease sensitivity; however, a general disruption of the active site structure especially upon Trp → Ala substitutions could not be ruled out.

Catalytic Mechanism. The mechanism for the ADPRT reaction catalyzed by ETA has previously been proposed and proceeds through an ordered sequential kinetic scheme (Chung & Collier, 1977; Bell & Eisenberg, 1996) in which the NAD^+ binds initially forming a binary complex that then binds eEF-2 (McGowan *et al*., 1991). A number of side chains within the active site cleft have been proposed to contribute key roles to the overall stability of bound NAD^+ (Bell & Eisenberg, 1996; Li *et al*., 1996; Gerry Prentice, unpublished observation). These residues are based on the two recent X-ray structures for ETA (Li *et al*., 1995, 1996) and for DT (Bell & Eisenberg, 1996) and on our modeling studies described herein. Our results indicate that Trp 466 may play a minor role in the catalytic mechanism and/or serve to provide the proper conformation of the NAD^+ binding pocket. With regard to the latter possibility, in the peptide scaffolding that comprises this binding pocket, Trp 466 is wedged in between a peptide segment composed of Leu 518−Ala 520 and another composed of Ala 523−Val 527. Additionally, extensive nonpolar interactions are evident between aliphatic and branched protein side chains with the phenyl moiety of the Trp 466 indole ring. Conservative substitution of Trp 466 with Phe leads to a only a 20-fold decrease in reaction rate, suggesting that Phe can substitute reasonably well for Trp at this position. In contrast, replacement of Trp 558 with Phe has an even smaller effect (3- and 5-fold decrease in k_{cat} and SpC, respectively). Inspection of the X-ray structures of both ETA and DT complexed with NAD^+ or its hydrolysis products suggests that Trp 558 may participate in NAD^+ binding; however, it can be replaced with Phe with only a marginal effect on the K_s value for substrate binding and on the GH activity, which suggests that productive binding of substrate does occur in this mutant protein. Therefore, Trp 558 likely serves to provide a nonpolar contact at which at least part of the adenine ring of NAD^+ docks (C-2 and C-3 of adenine faces the C-5 and C-6 of indole of Trp 558).

The ADPRT reaction likely proceeds by an S_N1 mechanism despite the observed inversion of configuration for the glycosidic bond of ribosyl diphthamide as determined by NMR spectroscopy (Oppenheimer & Bodley, 1981). Studies on substituent effects on the hydrolysis of 2′-substituted nicotinamide arabinosides (Handlon & Oppenheimer, 1991) indicate that the mechanism likely involves the formation of a oxocarbocationic intermediate, implying a S_N1 attack with characteristic first-order reaction kinetics (Buckley *et al*., 1994). The observation of an inversion of configuration (β to α) for the C−N bond in ribosyldiphthamide (Oppenheimer & Bodley, 1981) can best be explained by a restriction in the accessibility of the C-1 of the nicotinamide ribose to nucleophilic attack by the N-1 of the diphthamide imidazole, resulting in a back-side attack of the oxocarbonium ion. However, there is presently no structural information on the stereochemistry of this attack in the absence of a ternary complex consisting of NAD^+−ETA−eEF-2.

ACKNOWLEDGMENT

We thank Dr. Ira Pastan for kindly providing us with the plasmid pmS8 for production of wild-type PE40. We also thank Dr. David Eisenberg for the X-ray atomic coordinates for the DT−NAD^+ structure. Also, we are indebted to Dr. David McKay for the X-ray atomic coordinates of the partially refined (2.7 Å) whole ETA toxin structure.

REFERENCES

Allured, V. S., Collier, R. J., Carroll, S. F., & McKay, D. B. (1986) *Proc. Natl. Acad. Sci. U.S.A. 83*, 1320−1324.
Beattie, B. K., & Merrill, A. R. (1996) *Biochemistry 35*, 9042−9051.
Bell, C. E., & Eisenberg, D. (1996) *Biochemistry 35*, 1137−1149.
Bennett, M. J., Choe, S., & Eisenberg, D. (1994) *Protein Sci. 3*, 1444−1463.
Buckley, N., Handlon, A. L., Malby, D., Burlingame, A. L., & Oppenheimer, N. J. (1994) *J. Org. Chem. 59*, 3609−3615.
Carroll, S. F., & Collier, R. J. (1987) *J. Biol. Chem. 262*, 8707−8711.
Carroll, S. F., & Collier, R. J. (1988) *Methods Enzymol. 165*, 218−225.
Chung, D. W., & Collier, R. J. (1977) *Biochim. Biophys. Acta 483*, 248−257.
Clarke, A. J. (1987) *Biochim. Biophys. Acta 912*, 424−431.
Creed, D. (1984) *Photochem. Photobiol. 39*, 537−562.
Domenighini, M., Montecucco, C., Ripka, W. C., & Rappuoli, R. (1991) *Mol. Microbiol. 5*, 23−31.
Gill, S. C., & von Hippel, P. H. (1989) *Anal. Biochem. 182*, 319−326.
Handlon, A. L., & Oppenheimer, N. J. (1991) *J. Org. Chem. 56*, 5009−5010.
Iglewski, B. H., Liu, P. V., & Kabat, D. (1977) *Infect. Immun. 15*, 138−144.

Kandel, J., Collier, R. J., & Chung, D. W. (1974) *J. Biol. Chem. 249*, 2088−2097.
Killeen, K. P., & Collier, R. J. (1992) *Biochim. Biophys. Acta 1138*, 162−166.
Kondo, T., FitzGerald, D., Chaudhary, V. K., Adhya, S., & Pastan, I. (1988) *J. Biol. Chem. 263*, 9470−9475.
Laemmli, U. K. (1970) *Nature (London) 227*, 680−685.
Li, M., Dyda, F., Benhar, I., Pastan, I., & Davies, D. (1995) *Proc. Natl. Acad. Sci. U.S.A. 92*, 9308−9312.
Li, M., Dyda, F., Benhar, I., Pastan, I., & Davies, D. (1996) *Proc. Natl. Acad. Sci. U.S.A. 93*, 6902−6906.
Liu, P. V. (1973) *J. Infect. Dis. 128*, 506−513.
McGowan, J. L., Kessler, S. P., Anderson, D. C., & Galloway, D. R. (1991) *J. Biol. Chem. 266*, 4911−4916.
Michel, A., & Dirkx, J. (1977) *Biochim. Biophys. Acta 491*, 286−295.
Nilsson, L., & Nygaard, O. (1984) *Biochim. Biophys. Acta 782*, 49−54.
Oppenheimer, N. J., & Bodley, J. W. (1981) *J. Biol. Chem. 256*, 8579−8581.
Permyakov, E. A. (1993) in *Luminescent Spectroscopy of Proteins*, CRC Press, Boca Raton, FL.
Rasper, D. M., & Merrill, A. R. (1994) *Biochemistry 33*, 12981−12989.
Spande, T. F., & Witkop, B. (1967) *Methods Enzymol. 11*, 498−508.
Steer, B. A., & Merrill, A. R. (1995) *Biochemistry 34*, 7225−7233.
Vasil, M. L. (1986) *J. Pediatr. 108*, 800−805.
Wilson, B. A., & Collier, R. J. (1992) *Curr. Top. Microbiol. Immunol. 175*, 1−38.
Wilson, B. A., Reich, K. A., Weinstein, B. R., & Collier, R. J. (1990) *Biochemistry 29*, 8643−8651.
Wilson, B. A., Blanke, S. R., Reich, K. A., & Collier, R. J. (1994) *J. Biol. Chem. 269*, 23296−23301.

BI961985T